

Electronic Supplementary Information

Dual functional analytical device for self-powered point of care testing and electric energy storage

Chaomin Gao, Yanhu Wang, Min Su, Lina Zhang, Xianrang Song and Jinghua Yu*

Reagents and apparatus

Titanium foils (0.1 mm thickness, 99.6 % purity, Goodfellow, England) were purchased from Aldrich. Acetone, glucose, $\text{CuSO}_4 \cdot 5\text{H}_2\text{O}$, NaOH, and lactic acid were of analytical grade from Beijing Chemical Reagent Company (China) without further purification. Prostate-specific antigen (PSA) and the primary anti-PSA (Ab_1) were gotten from Linc-Bio Science Co. Ltd. (Shanghai, China). Ethylene glycol and ammonium fluoride (NH_4F) were purchased from Alfa Aesar China Ltd. Bilirubin oxidase (BOD) (E.C.1.10.3.2, 6 $\text{U} \cdot \text{mg}^{-1}$), Bovine serum albumin (BSA) and chloroauric acid ($\text{HAuCl}_4 \cdot 3\text{H}_2\text{O}$) were obtained from Sigma Chemical Co. (St Louis, MO, USA). Blocking buffer for blocking the residual reactive sites on the antibody was pH 7.4 phosphate buffer solution (PBS) containing 0.5 % BSA. A 0.10 M phosphate buffer solution (PBS, pH 7.4) consisting of KH_2PO_4 and Na_2HPO_4 was employed as the supporting electrolyte. Ultrapure water obtained from a Millipore water purification system ($\geq 18.2 \text{ M}\Omega \cdot \text{cm}$, Milli-Q, Millipore) was used in all assays and solutions. All other chemicals were of analytical grade and the solutions were prepared with the ultrapure water.

All electrochemical immunoassays were made with a CHI 760D electrochemical workstation (Shanghai Chenhua Instrument Corporation, China). Scanning electron microscope (SEM) analyses were recorded using a QUANTA FEG 250 thermal field emission scanning electron microscopy (FEI Co, USA), and the microscope was equipped with an Oxford X-MAX50 energy dispersive spectrometer (EDS) (Oxford, Britain). The phase characterization was performed

by X-ray diffraction (XRD) using a D8 advance diffractometer system equipped with Cu K α radiation (Bruker Co, Germany).

Preparation of the TNTs, Cu₂O-TNTs, AuNPs-TNTs and all-solid-state Ti supercapacitor.

The electrochemical anodic oxidation technique was used to fabricate the highly ordered TiO₂ nanotubes (TNTs) array electrode according to previous work.¹ TNTs were fabricated through a two-step anodization. The Ti foil was rinsed with acetone and ultrapure water for 10 min then was dried with pure N₂ at room temperature before anodization. In the first step, anodization was carried out in ethylene glycol electrolyte containing 0.5 wt % NH₄F and 2 wt % H₂O. The voltage and oxidation time were 20 V and 1 h, respectively. Then the cleaned Ti foil was soaked in a mixture of HF and HNO₃ acids for 1 min (the mixing ratio of HF/HNO₃/H₂O was 1:4:5 in volume and the mixing was dangerous). After that, the cleaned Ti foil was used for the secondary anodization in hydrofluoric acid (0.5 wt %). A potential of 20 V was used in this experiment. Anodized Ti foil was annealed in a dry oxygen environment at 500 °C for 1 h; heating and cooling rates were kept at 2.5 °C·min⁻¹.

Cu₂O-TNTs composites were prepared by electrochemical deposition of Cu₂O in a three-electrode cell, using the TNTs, Ag/AgCl (saturated KCl), and platinum foil as the working, reference, and counter-electrodes, respectively. A CHI 760D electrochemical working station (ChenHua Instruments Co. Ltd., Shanghai, China) was used as the power source. The electrolyte was obtained by dissolving 1 mol·L⁻¹ CuSO₄ in a 3 mol·L⁻¹ lactic acid solution to form a copper lactate complex, and pH was further adjusted to 12 using 5 M NaOH solution. The electrolyte was stirred and kept at a constant temperature of 35 °C. An electrodeposition charge of 1 C and a potential of -0.7 V versus Ag/AgCl electrode were used during the deposition process. After the electrochemical deposition, the Ti foil covered with Cu₂O-TNTs was thoroughly washed using ultrapure water, and air dried.

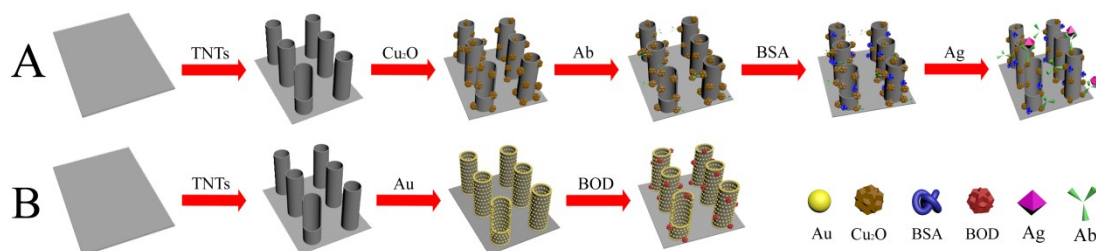
The AuNPs-TNTs electrode was prepared according to previous work ² and could be described as below. A novel photoelectrochemical deposition method was exploited to modify the resulting nanotubes with AuNPs. The TNTs served as the working electrode in a conventional photoelectrochemical cell. An Ag/AgCl (saturated KCl) electrode and a platinum electrode served as the reference and counter electrode, respectively. The photoelectrochemical deposition of AuNPs was carried out by cyclic voltammetry with a potential range from 0.0 to +1.4 V for 30 min under the irradiation of light at 365 nm wavelength. The photoelectroplating solution was prepared by dissolving H₂AuCl₄·3H₂O (0.1 mM) in H₂SO₄ solution (0.5 M).

The all-solid-state Ti supercapacitor was fabricated directly on the TNTs with a simple approach, that is, soaking and curding of the as-prepared TNTs in the H₃PO₄-poly (vinyl alcohol) (PVA) gel electrolyte.³ The detailed procedure was described as follows: firstly, the solution of H₃PO₄-PVA gel electrolyte was successfully prepared by mixing 10 g PVA powder activated with ethanol, 10 g H₃PO₄ and 100 mL ultrapure water together and heated to 85 °C until the solution became clear. Then the solution was remained in an ambient condition. Subsequently, the TNTs was immersed into the hot solution of H₃PO₄-PVA gel electrolyte for 10 min and then picked out. When the electrolyte became cool down, the viscosity would increase a lot, which would not be in favor of the thorough soakage of the H₃PO₄-PVA gel electrolyte into the TNTs, so the TNTs was immersed in the hot solution.

Fabrication of BFC based self-powered sensor

The construction procedures of the BFC based self-powered sensor are shown in Scheme S1, and the details are described below. The Ab₁ was immobilized into the Cu₂O-TNTs anode via physical adsorption. Briefly 20 μL of 100 μg·mL⁻¹ Ab₁ solution was added onto the Cu₂O-TNTs anode and then the device was incubated at 4 °C for 1 h. Then the blocking solution containing 0.5 % BSA (pH 7.4) which served to block the possible remaining active sites against

nonspecific adsorption was added into the electrode and incubated for 1 h at room temperature. Here, BSA was served to block the nonspecific binding sites in Ab₁-Cu₂O-TNTs anode. The cathode was fabricated as follows. Briefly, the AuNPs-TNTs electrode was immersed in a solution containing 1.0 U·mg⁻¹ BOD solution of 100 mM PBS (pH 7.4) for 2 h at room temperature. The as-prepared electrode was denoted as BOD-AuNPs-TNTs cathode.



Scheme S1 Schematic diagram of the fabrication of the anode (A) and cathode (B) of the BFC based self-powered sensor.

EIS of the modified anode and cathode

Electrochemical impedance spectroscopy (EIS) was an effective and convenient method for monitoring the changes in the surface features of the modified electrodes in the assembly processes and the EIS of the resulting anode and cathode were given in Fig. S1. Each reaction step of the modified electrode was analyzed by EIS in the frequency range 100 MHz to 10 KHz at a bias potential of 170 mV (vs Ag/AgCl), and in a PBS (0.1 M, pH 7.4) containing 10 mM $[\text{Fe}(\text{CN})_6]^{3-/4-}$ as probe. Note that the diameters of the semicircles were equal to the charge-transfer resistance (R_{et}).⁴ As shown in Fig. S1A, the bare TiO₂ electrode exhibited a high R_{et} of the redox couple (curve a). Compared with the TiO₂ electrode, The Cu₂O-TNTs electrode showed a high resistance for the redox probe (curve b), which implied that the Cu₂O nanoparticles may hinder the electron transfer and also demonstrates that the Cu₂O nanoparticles had been successfully deposited on the TNTs. A remarkable increase in the R_{et} value was observed after the immobilization of Ab₁ onto the Cu₂O-TNTs anode, indicating that the protein molecule with low conductivity acted as a definite kinetic barrier for the electron transfer (curve c). Then, the R_{et} continue increased after BSA was

dropped on the electrode to block the active site (curve d). Further binding of PSA standard solution hindered the interfacial electron transfer of the $[\text{Fe}(\text{CN})_6]^{3-/4-}$ pair, which resulted in the R_{et} further increase (curve e).

Meanwhile, the AuNPs-TNTs cathode showed a much lower resistance for the redox probe (Fig. S1B curve a) compared with bare TNTs (Fig. S1B curve b), which implied that the AuNPs greatly accelerated the electron transfer and also demonstrated that the AuNPs had been successfully deposited in the TNTs. After the attachment of BOD gave rise to an additional barrier towards the access of the redox probe to the AuNPs-TNTs cathode (Fig. S1B curve c), which resulted in a further increase in the R_{et} .⁵

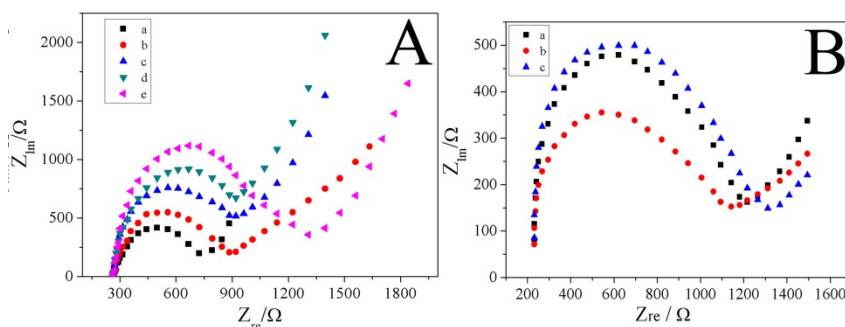


Fig. S1 (A) EIS of the anode under different condition in 10.0 mM $[\text{Fe}(\text{CN})_6]^{3-/4-}$ solution containing 0.5 M KCl. a) bare TNTs, b) Cu_2O -TNTs, c) Ab_1 modified Cu_2O -TNTs, d) after the absorption of BSA, e) after the addition of PSA; (B) EIS of the cathode under different condition in 10.0 mM $[\text{Fe}(\text{CN})_6]^{3-/4-}$ solution containing 0.5 M KCl. a) bare TNTs, b) AuNPs-TNTs, c) after the immobilization of BOD.

Electrochemical characterization of the modified anode

To evaluate the performance of $\text{Ab}/\text{BSA}/\text{PSA}$ modified anode, a conventional three-electrode setup, with modified anode as working electrode, Ag/AgCl electrode (saturated KCl) as reference electrode and platinum wire as counter electrode, was constructed in phosphate buffer solution (pH 7.4) with the presence of 40 mM glucose. Fig. S2 showed the cyclic voltammetry (CV) response of the modified anode recorded in phosphate buffer solution (pH 7.4) with the presence of 40 mM glucose. As was seen from Fig. S2, when $\text{Ab}_1/\text{BSA}/\text{Ag}$ was progressively dropped onto the Cu_2O -TNTs electrode, the glucose could also be oxidized, generating weak current. However, the redox current decreased remarkably compared with Cu_2O -TNTs electrode (curve a).

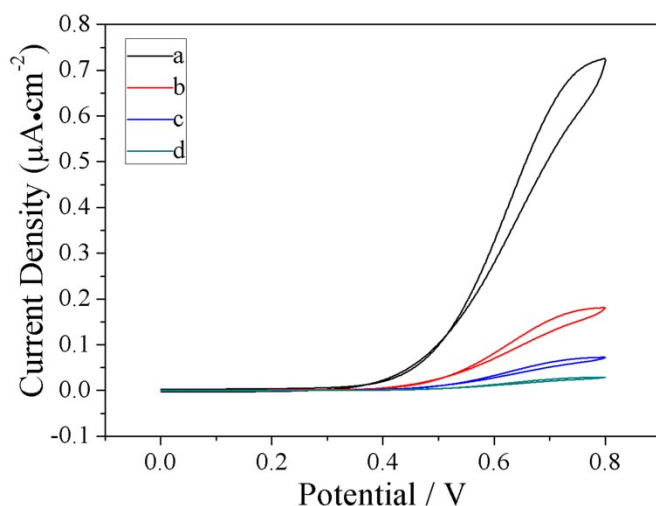


Fig. S2 CVs of Cu₂O-TNTs (curve a), Ab₁-Cu₂O-TNTs (curve b), BSA-Ab₁-Cu₂O-TNTs (curve c) and PSA-BSA-Ab₁-Cu₂O-TNTs (curve d) in the presence of 40 mM glucose.

Optimization of the Immunoassay Conditions

In this work, the glucose was used as fuel of the BFC based self-powered sensor, and the concentration of glucose could influence the performance of BFC. The optimization procedures were performed at room temperature and consistent to the assay procedures containing 10 ng·mL⁻¹. And the effects of the concentration of glucose on the current intensity of this BFC were investigated as follows. As shown in Fig. S3A, the current intensity increased gradually with the increasing of glucose concentration, however, when the concentration of glucose was higher than 40 mM no obvious increase in current intensity was obtained. Therefore, the 40 mM was selected as the optimal concentration and used in the further study. The incubation time was another critical parameter that affected the analytical performance and the efficiency of the immunoassay. At room temperature, the current response decreased with increasing incubation time and then stabilized at 30 min (Fig. S3B), indicating the maximum formation of the immunoreaction. The optimal incubation time of PSA immune-complexes was 30 min, and accordingly, an incubation time of 30 min was selected for the subsequent experiments. The pH of the detection solution was another important factor in the immune reaction. As shown in Fig. S3C, the current response increased as the pH value increased from 6.0 to 7.4 and then decreased as pH

values higher than 7.4. Thus, PBS at pH 7.4 was selected for preparing the solutions used for detection.

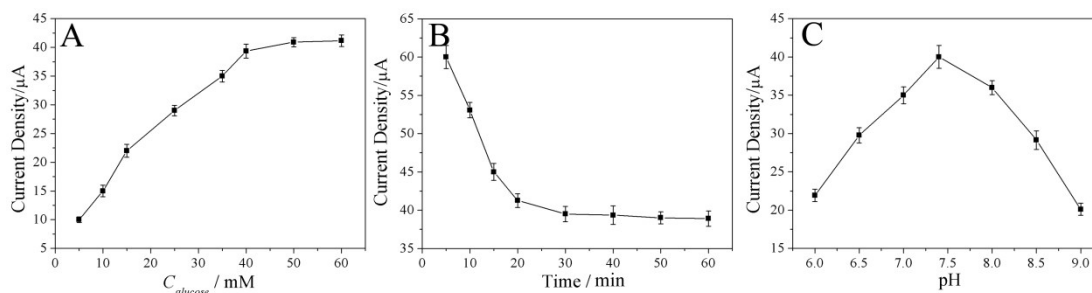


Fig. S3 (A) Effect of glucose concentration on current response; (B) The effect of incubation time on current intensity at $10 \text{ ng} \cdot \text{mL}^{-1}$ PSA concentration; (C) Effect of pH value on current intensity.

Selectivity, reproducibility and stability of this self-powered sensor

Fig. S4 showed the selectivity of the proposed BFC based self-powered sensor by the use of the carcinoembryonic antigen (CEA), human IgG (HIgG), α -fetoprotein (AFP) and human serum albumin (HSA), as interfering agents. The results suggested that these interfering agents lead to almost no signal increase and thus a satisfactory selectivity.

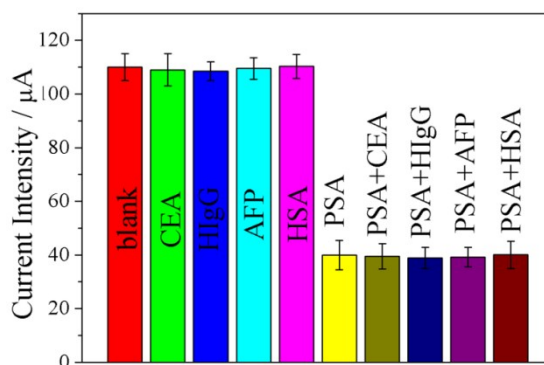


Fig. S4 Specificity of this self-powered sensor towards PSA.

The reproducibility of this self-powered sensor was investigated with intra-assay and inter-assay. And the intra-assay RSD obtained were 4.6, 5.1 and 6.7 % at PSA concentration 1, 50 and $100 \text{ ng} \cdot \text{mL}^{-1}$. While, the inter-assay RSD were 4.9, 5.5 and 7.2 % that obtained by measuring the same samples with five sensors prepared independently under identical experimental conditions. The results suggested that the good precision and reproducibility of the as-prepared sensor.

To investigate the stability of this self-powered sensor, the proposed sensor was stored at 4 °C, and measured at intervals of a week; no obvious change was observed after 1 months. These results indicated that this self-powered sensor had good stability and was fairly robust in normal storage conditions and achieved sufficient stability and precision during manufacture, storage, or long-distance transport to remote regions and developing countries.

References

- 1 W. Zhu, Y. An, X. Luo, F. Wang, J. Zheng, L. Tang, Q. Wang, Z. Zhang, W. Zhang, L. Jin, *Chem. Commun.*, 2009, 2682-2684.
- 2 Y. R. An, L. L Tang, X. L. Jiang, H. Chen, M. C. Yang, L. T. Jin, S. P. Zhang, C. G. Wang, and W. Zhang, *Chem. Eur. J.*, 2010, **16**, 14439-14446.
- 3 S. J. Guo, Y. X. Fang, S. J. Dong and E. K. Wang, *Inorg. Chem.*, 2007, **46**, 9537-9539.
- 4 Y. Zhang, H. Wang, J. F. Nie, Y. W. Zhang, G. L. Shen and R. Q. Yu, *Biosens. Bioelectron.*, 2009, **25**, 34-40.
- 5 A. Korani, A. Salimi, *Biosens. Bioelectron.*, 2013, **50**, 186-193.